

李伟华,刘清华,赵成刚. 饱和多孔介质三维时域黏弹性人工边界与动力反应分析的显式有限元法. 地球物理学报, 2010, **53**(10):2460~2469, DOI:10.3969/j.issn.0001-5733.2010.10.020

Li W H, Liu Q H, Zhao C G. Three-dimensional viscous-spring boundaries in time domain and dynamic analysis using explicit finite element method of saturated porous medium. *Chinese J. Geophys.* (in Chinese), 2010, **53**(10):2460~2469, DOI:10.3969/j.issn.0001-5733.2010.10.020

饱和多孔介质三维时域黏弹性人工边界与动力反应分析的显式有限元法

李伟华¹, 刘清华^{1,2}, 赵成刚¹

1 北京交通大学土木工程学院, 北京 100044

2 北京军区 66469 部队, 北京 100042

摘 要 本文基于 Biot 的饱和多孔介质本构方程, 考察具有辐射阻尼的外行球面波, 推导了饱和多孔介质三维黏弹性人工边界的法向和切向边界方程; 在已有的饱和多孔介质二维显式有限元数值计算方法基础上, 提出该理论的三维方法, 并开发了实现该三维方法的有限元程序. 算例表明饱和多孔介质三维时域黏弹性人工边界与动力反应分析的显式有限元法具有较好的精度和稳定性.

关键词 饱和多孔介质, 三维黏弹性动力人工边界, 有限元法

DOI:10.3969/j.issn.0001-5733.2010.10.020

中图分类号 P631

收稿日期 2009-11-24, 2010-09-25 收修定稿

Three-dimensional viscous-spring boundaries in time domain and dynamic analysis using explicit finite element method of saturated porous medium

LI Wei-Hua¹, LIU Qing-Hua^{1,2}, ZHAO Cheng-Gang¹

1 School of Civil Engineering, Beijing Jiao-tong University, Beijing 100044, China

2 Militaryarea of Beijing, Unit 66469, Beijing 100042, China

Abstract Based on Biot's dynamic theory for saturated porous media and the constitutive equations of poro-elastic media, this paper discusses the normal and tangential stress formulae on the artificial boundary of sphere shapes under the assumption of out-going spherical waves, and constitutes the three-dimensional viscous-spring boundaries in time domain for saturated porous media; According to the dynamic analysis of saturated porous media by using explicit finite element method, this paper develops the finite element method that could solve the three-dimensional problems, and develops finite element program. The analysis of the saturated porous medium dynamic response indicates that the combination method of the explicit finite element method and the three-dimensional viscous-spring boundary enjoy good accuracy and good stability.

Keywords Saturated porous media, Three-dimensional viscous-spring artificial boundary, Finite element method

基金项目 国家自然科学基金重大研究计划项目(90715035), 国家自然科学基金项目(50708005), 北京市教委重点项目(KZ200910005002)及中央高校基本科研业务费专项资金项目(2009JBM064)资助.

作者简介 李伟华, 女, 1976 年生, 博士, 副教授, 主要从事土动力学与地震工程方面的研究工作. E-mail: whli@bjtu.edu.cn

1 引言

地震波在从震源通过各种途径传播时,通常要穿过饱和土层和非饱和土层最后到达地面,地壳上部的连续固体骨架中包含着相互连通的孔隙和槽路,当将充满液体的土层进行动力分析时,按饱和多孔介质理论比按单相介质理论分析更为合理.与单相介质相比,饱和多孔介质中的波动问题要复杂得多,近年来饱和多孔介质人工边界及其数值模拟问题受到越来越多学者的重视. Modaresi 等^[1]首先将人工边界上的 $u-p$ 表达式引入饱和多孔介质的有限元分析中; Degrande 等^[2]通过引入势函数、波场分解以及 Fourier 变换给出人工边界上频域内的应力和位移的表达式,实际上是 DtN 边界在法向上的表示; Akiyoshi 等^[3]通过波场分解和 Fourier 变换得到频域内固、液相位移、总应力和流体压力的表达式,利用旁轴近似和 Fourier 反变换得到人工边界上应力与 $u-p$ 、 $u-U$ 、 $u-W$ 的黏性边界表达形式; Gajo^[4]建立两种极端情形下(即黏性耦合很小和很大时的情形)饱和介质一维单侧波动方程,得到类似单相介质的黏性边界,然后根据 Higdon 的方法,得到高阶多向人工边界条件; Akiyoshi 等^[5]采用等效拉梅常数和平均渗透系数,通过线性变换,将各向异性波动方程等效为各向同性,又将此边界推广为考虑各向异性的人工边界;邵秀民等^[6]基于透射边界,提出一种饱和介质的人工边界条件,并将其应用到二维有限元计算分析中; Zerfa^[7]根据 Bowen 的公式^[8]提出可考虑排水特性的黏性人工边界;刘光磊、宋二祥^[9]根据 Biot 动力固结理论外行柱面波假设,提出了一种适用于饱和多孔介质时域动力分析的二维黏弹性边界条件;王子辉、赵成刚等^[10]从二维平面外行柱面波出发,提出了一种饱和多孔介质黏弹性动力人工边界.杜修力、李立云^[11]采用平面波和远场散射波经验叠加来反映外行波传播,并在推导过程中考虑了多角度透射的影响,提出了饱和多孔介质近场波动分析的一种黏弹性人工边界处理方法.

上述研究中,多数是针对二维问题展开的,有关饱和多孔介质的三维动力人工边界及其数值模拟的研究并不多见.本文基于饱和多孔介质波动理论,采用与文献^[10]类似的思路提出饱和多孔介质三维黏弹性动力人工边界处理方法,同时根据本文作者已

建立的饱和多孔介质二维显式有限元数值计算方法^[12],提出该理论的三维数值模拟方法,并开发了实现该三维方法的有限元程序.最后将建立的人工边界条件和饱和多孔介质三维动力反应分析的显式有限元法相结合,用于饱和多孔介质的动力研究.

2 饱和多孔介质三维显式有限元方程的建立

Biot^[13]提出了饱和多孔介质的波动方程

$$\begin{aligned} & \mu \nabla^2 \mathbf{u} + \nabla [(\lambda + \mu)e + Q\epsilon] = \\ & \left(\rho_{11} \frac{\partial^2 \mathbf{u}}{\partial t^2} + \rho_{12} \frac{\partial^2 \mathbf{U}}{\partial t^2} \right) + b \left(\frac{\partial \mathbf{u}}{\partial t} - \frac{\partial \mathbf{U}}{\partial t} \right) \\ & \nabla [Qe + R\epsilon] = \left(\rho_{12} \frac{\partial^2 \mathbf{u}}{\partial t^2} + \rho_{22} \frac{\partial^2 \mathbf{U}}{\partial t^2} \right) - b \left(\frac{\partial \mathbf{u}}{\partial t} - \frac{\partial \mathbf{U}}{\partial t} \right), \end{aligned} \quad (1)$$

式中 λ, μ, Q, R 为弹性常数; $\rho_{11}, \rho_{22}, \rho_{12}$ 为动力质量系数, $\rho_{11} = (1-n)\rho_s + \rho_a$, $\rho_{22} = n\rho_f + \rho_a$, $\rho_{12} = -\rho_a$; ρ_s 和 ρ_f 分别为固体骨架和孔隙流体的质量密度, ρ_a 为描述流固两相耦合的附加质量密度; e 和 ϵ 分别表示固相骨架和孔隙流体的体积应变, $e = \text{div } \mathbf{u}$, $\epsilon = \text{div } \mathbf{U}$; b 为与渗流有关的系数, $b = \zeta n^2/k$, ζ 为流体滞变系数, n 为孔隙率, k 为渗透系数.

2.1 波动方程的矩阵表达形式

由式(1)可以得到该波动方程的矩阵表达式

$$\mathbf{L}^T \mathbf{D}_1 \mathbf{L} \mathbf{u} + \mathbf{L}^T \mathbf{D}_2 \mathbf{L} \mathbf{U} = \rho_{11} \ddot{\mathbf{u}} + \rho_{12} \ddot{\mathbf{U}} + b(\dot{\mathbf{u}} - \dot{\mathbf{U}}), \quad (2)$$

$$\mathbf{L}^T \mathbf{D}_2 \mathbf{L} \mathbf{u} + \mathbf{L}^T \mathbf{D}_3 \mathbf{L} \mathbf{U} = \rho_{12} \ddot{\mathbf{u}} + \rho_{22} \ddot{\mathbf{U}} - b(\dot{\mathbf{u}} - \dot{\mathbf{U}}), \quad (3)$$

其中

$$\mathbf{L}^T = \begin{bmatrix} \frac{\partial}{\partial x} & 0 & 0 & \frac{\partial}{\partial y} & 0 & \frac{\partial}{\partial z} \\ 0 & \frac{\partial}{\partial y} & 0 & \frac{\partial}{\partial x} & \frac{\partial}{\partial z} & 0 \\ 0 & 0 & \frac{\partial}{\partial z} & 0 & \frac{\partial}{\partial y} & \frac{\partial}{\partial x} \end{bmatrix},$$

$$\mathbf{u} = \begin{Bmatrix} u_x \\ u_y \\ u_z \end{Bmatrix}, \quad \mathbf{U} = \begin{Bmatrix} U_x \\ U_y \\ U_z \end{Bmatrix},$$

$$\mathbf{D}_1 = \begin{bmatrix} \lambda + 2\mu & \lambda & \lambda & & & \\ \lambda & \lambda + 2\mu & \lambda & & & \\ \lambda & \lambda & \lambda + 2\mu & & & \\ & & & \mu & 0 & 0 \\ & & & 0 & \mu & 0 \\ & & & 0 & 0 & \mu \end{bmatrix},$$

$$\mathbf{D}_2 = \begin{bmatrix} Q & Q & Q & & & \\ Q & Q & Q & 0 & & \\ Q & Q & Q & & & \\ & & & 0 & 0 & 0 \\ & & & & 0 & 0 & 0 \\ & & & & & 0 & 0 & 0 \end{bmatrix}, \mathbf{D}_3 = \begin{bmatrix} R & R & R & & & \\ R & R & R & 0 & & \\ R & R & R & & & \\ & & & 0 & 0 & 0 \\ & & & & 0 & 0 & 0 \\ & & & & & 0 & 0 & 0 \end{bmatrix}.$$

2.2 建立有限元方程的列式

设 \mathbf{N} 为单元形函数矩阵, 则

$$\mathbf{u}^e = \mathbf{N}\mathbf{u}_e, \mathbf{U}^e = \mathbf{N}\mathbf{U}_e, \quad (4)$$

式中 \mathbf{u}_e 和 \mathbf{U}_e 分别为单元 e 的节点固相和液相位移; \mathbf{u}^e 和 \mathbf{U}^e 分别为单元 e 的固相和液相位移.

根据文献 [12], 方程 (2)、(3) 的局部节点系 GALERKIN 弱式为

$$\begin{aligned} & \sum_e \int_{\Omega^e} \mathbf{N}^T \rho_{11} \mathbf{N} \ddot{\mathbf{u}}_e \, dx dy dz + \sum_e \int_{\Omega^e} \mathbf{N}^T \rho_{12} \mathbf{N} \ddot{\mathbf{U}}_e \, dx dy dz + \sum_e \int_{\Omega^e} \mathbf{N}^T b \mathbf{N} (\dot{\mathbf{u}}_e - \dot{\mathbf{U}}_e) \, dx dy dz \\ & + \sum_e \int_{\Omega^e} \mathbf{B}^T \mathbf{D}_1 \mathbf{B} \mathbf{u}_e \, dx dy dz + \sum_e \int_{\Omega^e} \mathbf{B}^T \mathbf{D}_2 \mathbf{B} \mathbf{U}_e \, dx dy dz = \sum_e \int_{\Gamma^e} \mathbf{N}^T \mathbf{f}_{u_e} \, d\Gamma, \\ & \sum_e \int_{\Omega^e} \mathbf{N}^T \rho_{12} \mathbf{N} \ddot{\mathbf{u}}_e \, dx dy dz + \sum_e \int_{\Omega^e} \mathbf{N}^T \rho_{22} \mathbf{N} \ddot{\mathbf{U}}_e \, dx dy dz - \sum_e \int_{\Omega^e} \mathbf{N}^T b \mathbf{N} (\dot{\mathbf{u}}_e - \dot{\mathbf{U}}_e) \, dx dy dz \\ & + \sum_e \int_{\Omega^e} \mathbf{B}^T \mathbf{D}_2 \mathbf{B} \mathbf{u}_e \, dx dy dz + \sum_e \int_{\Omega^e} \mathbf{B}^T \mathbf{D}_3 \mathbf{B} \mathbf{U}_e \, dx dy dz = \sum_e \int_{\Gamma^e} \mathbf{N}^T \mathbf{f}_{U_e} \, d\Gamma, \end{aligned} \quad (5)$$

其中应变矩阵 $\mathbf{B} = \mathbf{L} \cdot \mathbf{N}$, \mathbf{L} 为三维问题的微分算子; \mathbf{f}_{u_e} 和 \mathbf{f}_{U_e} 分别为作用在单元 e 边界上的固相和液相外力.

2.3 离散方程及解耦方法

对于三维问题, 采用 8 节点六面体等参单元, 节点 i 和与其直接相邻的节点 k 所构成局部节点系, 此节点系中包含 27 个节点. 根据式 (5) 可以直接得到如下离散公式

$$\left. \begin{aligned} & \sum_{L=1}^8 \sum_{j=1}^8 \mathbf{M}_{ij}^L \ddot{\mathbf{u}}_j^L + \sum_{L=1}^8 \sum_{j=1}^8 \widetilde{\mathbf{M}}_{uUij}^L \ddot{\mathbf{U}}_j^L + \sum_{L=1}^8 \sum_{j=1}^8 \mathbf{C}_{ij}^L (\dot{\mathbf{u}}_j^L - \dot{\mathbf{U}}_j^L) + \sum_{L=1}^8 \sum_{j=1}^8 \mathbf{K}_{uij}^L \mathbf{u}_j^L + \sum_{L=1}^8 \sum_{j=1}^8 \mathbf{K}_{uUij}^L \mathbf{U}_j^L = \sum_{L=1}^8 \mathbf{f}_{u_i}^L \\ & \sum_{L=1}^8 \sum_{j=1}^8 \widetilde{\mathbf{M}}_{uUij}^L \ddot{\mathbf{u}}_j^L + \sum_{L=1}^8 \sum_{j=1}^8 \mathbf{M}_{Uij}^L \ddot{\mathbf{U}}_j^L - \sum_{L=1}^8 \sum_{j=1}^8 \mathbf{C}_{ij}^L (\dot{\mathbf{u}}_j^L - \dot{\mathbf{U}}_j^L) + \sum_{L=1}^8 \sum_{j=1}^8 \mathbf{K}_{Uij}^L \mathbf{u}_j^L + \sum_{L=1}^8 \sum_{j=1}^8 \mathbf{K}_{UUij}^L \mathbf{U}_j^L = \sum_{L=1}^8 \mathbf{f}_{U_i}^L \end{aligned} \right\}, \quad (6)$$

式中, L 代表节点 i 周围的不同单元, 因只有节点 i 周围 8 个单元对其有影响, 所以只给出 8 个单元的求和, j 代表同一单元内的 8 个节点. 波动问题数值模拟的精度要求有限元的尺寸同波长相比应足够小, 故在每一单元内惯性力的空间变化很小, 可在一个单元内的加速度为常量, 即等于其节点的加速度, $\ddot{\mathbf{u}}_j^L = \ddot{\mathbf{u}}_i$, $\ddot{\mathbf{U}}_j^L = \ddot{\mathbf{U}}_i$, 由此得到集中质量阵. 根据集中质量矩阵有

$$\mathbf{M}_{u_i} \ddot{\mathbf{u}}_i = \sum_{L=1}^8 \sum_{j=1}^8 \mathbf{M}_{ij}^L \ddot{\mathbf{u}}_j^L, \mathbf{M}_{U_i} \ddot{\mathbf{U}}_i = \sum_{L=1}^8 \sum_{j=1}^8 \mathbf{M}_{Uij}^L \ddot{\mathbf{U}}_j^L, \widetilde{\mathbf{M}}_{uU_i} \ddot{\mathbf{u}}_i = \sum_{L=1}^8 \sum_{j=1}^8 \widetilde{\mathbf{M}}_{uUij}^L \ddot{\mathbf{u}}_j^L, \quad (7a)$$

其中,

$$\mathbf{M}_{u_i} = \sum_{L=1}^8 \sum_{j=1}^8 \mathbf{M}_{ij}^L, \mathbf{M}_{U_i} = \sum_{L=1}^8 \sum_{j=1}^8 \mathbf{M}_{Uij}^L, \widetilde{\mathbf{M}}_{uU_i} = \sum_{L=1}^8 \sum_{j=1}^8 \widetilde{\mathbf{M}}_{uUij}^L. \quad (7b)$$

式 (6)、(7) 中,

$$\begin{aligned} \mathbf{M}_{ij}^L &= \iiint_{\Omega^L} \rho_{11} \mathbf{N}_i \mathbf{N}_j \, dx dy dz = \int_{-1}^1 \int_{-1}^1 \int_{-1}^1 \rho_{11} \mathbf{N}_i \mathbf{N}_j |\mathbf{J}| \, d\xi d\eta d\zeta, \\ \mathbf{M}_{Uij}^L &= \iiint_{\Omega^L} \rho_{22} \mathbf{N}_i \mathbf{N}_j \, dx dy dz = \int_{-1}^1 \int_{-1}^1 \int_{-1}^1 \rho_{22} \mathbf{N}_i \mathbf{N}_j |\mathbf{J}| \, d\xi d\eta d\zeta, \\ \widetilde{\mathbf{M}}_{uUij}^L &= \iiint_{\Omega^L} \rho_{12} \mathbf{N}_i \mathbf{N}_j \, dx dy dz = \int_{-1}^1 \int_{-1}^1 \int_{-1}^1 \rho_{12} \mathbf{N}_i \mathbf{N}_j |\mathbf{J}| \, d\xi d\eta d\zeta, \\ \mathbf{C}_{ij}^L &= \iiint_{\Omega^L} b \mathbf{N}_i \mathbf{N}_j \, dx dy dz = \int_{-1}^1 \int_{-1}^1 \int_{-1}^1 b \mathbf{N}_i \mathbf{N}_j |\mathbf{J}| \, d\xi d\eta d\zeta, \\ \mathbf{K}_{uij}^L &= \int_{-1}^1 \int_{-1}^1 \int_{-1}^1 \mathbf{B}_i^T \mathbf{D}_1 \mathbf{B}_j |\mathbf{J}| \, d\xi d\eta d\zeta, \\ \mathbf{K}_{uUij}^L &= \mathbf{K}_{Uij}^L = \int_{-1}^1 \int_{-1}^1 \int_{-1}^1 \mathbf{B}_i^T \mathbf{D}_2 \mathbf{B}_j |\mathbf{J}| \, d\xi d\eta d\zeta, \end{aligned}$$

$$\mathbf{K}_{Uij}^L = \int_{-1}^1 \int_{-1}^1 \int_{-1}^1 \mathbf{B}_i^T \mathbf{D}_3 \mathbf{B}_j |J| d\xi d\eta d\zeta,$$

$$\mathbf{f}_{ui}^L = \int_{\Gamma^L} \mathbf{N}_i \cdot \tilde{\mathbf{T}}_s d\Gamma, \mathbf{f}_{Ui}^L = \int_{\Gamma^L} \mathbf{N}_i \begin{Bmatrix} n\pi \\ n\pi \\ n\pi \end{Bmatrix} d\Gamma, \tilde{\mathbf{T}}_s = \begin{Bmatrix} \tilde{T}_x \\ \tilde{T}_y \\ \tilde{T}_z \end{Bmatrix}.$$

2.4 节点动力反应的显式表达

利用有限元方法建立离散的动力方程后,采用中心差分法与 Newmark 平均加速度近似格式相结合的方法求解节点动力方程式(6).

当 $t = p\Delta t$ 时刻,将式(7)代入式(6)得到 $p\Delta t$ 时刻 i 节点的运动方程:

$$\left. \begin{aligned} \mathbf{M}_{ui} \ddot{\mathbf{u}}_i^p + \tilde{\mathbf{M}}_{uUi} \ddot{\mathbf{U}}_i^p + \sum_{L=1}^8 \sum_{j=1}^8 \mathbf{C}_{ij}^L (\dot{\mathbf{u}}_j^{L,p} - \dot{\mathbf{U}}_j^{L,p}) + \sum_{L=1}^8 \sum_{j=1}^8 \mathbf{K}_{uij}^L \mathbf{u}_j^{L,p} + \sum_{L=1}^8 \sum_{j=1}^8 \mathbf{K}_{Uij}^L \mathbf{U}_j^{L,p} &= \sum_{L=1}^8 \mathbf{f}_{ui}^{L,p} \\ \tilde{\mathbf{M}}_{uUi} \ddot{\mathbf{u}}_i^p + \mathbf{M}_{Ui} \ddot{\mathbf{U}}_i^p - \sum_{L=1}^8 \sum_{j=1}^8 \mathbf{C}_{ij}^L (\dot{\mathbf{u}}_j^{L,p} - \dot{\mathbf{U}}_j^{L,p}) + \sum_{L=1}^8 \sum_{j=1}^8 \mathbf{K}_{Uij}^L \mathbf{u}_j^{L,p} + \sum_{L=1}^8 \sum_{j=1}^8 \mathbf{K}_{Uij}^L \mathbf{U}_j^{L,p} &= \sum_{L=1}^8 \mathbf{f}_{Ui}^{L,p} \end{aligned} \right\}, \quad (8)$$

在 $(p+1)\Delta t$ 时刻,将式(7)代入式(6),并与式(8)相加得到

$$\left. \begin{aligned} \mathbf{M}_{ui} (\ddot{\mathbf{u}}_i^p + \ddot{\mathbf{u}}_i^{p+1}) + \tilde{\mathbf{M}}_{uUi} (\ddot{\mathbf{U}}_i^p + \ddot{\mathbf{U}}_i^{p+1}) + \sum_{L=1}^8 \sum_{j=1}^8 \mathbf{C}_{ij}^L ((\dot{\mathbf{u}}_j^{L,p} + \dot{\mathbf{u}}_j^{L,p+1}) - (\dot{\mathbf{U}}_j^{L,p} + \dot{\mathbf{U}}_j^{L,p+1})) \\ + \sum_{L=1}^8 \sum_{j=1}^8 \mathbf{K}_{uij}^L (\mathbf{u}_j^{L,p} + \mathbf{u}_j^{L,p+1}) + \sum_{L=1}^8 \sum_{j=1}^8 \mathbf{K}_{Uij}^L (\mathbf{U}_j^{L,p} + \mathbf{U}_j^{L,p+1}) &= \sum_{L=1}^8 (\mathbf{f}_{ui}^{L,p} + \mathbf{f}_{ui}^{L,p+1}) \\ \mathbf{M}_{uUi} (\ddot{\mathbf{u}}_i^p + \ddot{\mathbf{u}}_i^{p+1}) + \tilde{\mathbf{M}}_{Ui} (\ddot{\mathbf{U}}_i^p + \ddot{\mathbf{U}}_i^{p+1}) - \sum_{L=1}^8 \sum_{j=1}^8 \mathbf{C}_{ij}^L ((\dot{\mathbf{u}}_j^{L,p} + \dot{\mathbf{u}}_j^{L,p+1}) - (\dot{\mathbf{U}}_j^{L,p} + \dot{\mathbf{U}}_j^{L,p+1})) \\ + \sum_{L=1}^8 \sum_{j=1}^8 \mathbf{K}_{Uij}^L (\mathbf{u}_j^{L,p} + \mathbf{u}_j^{L,p+1}) + \sum_{L=1}^8 \sum_{j=1}^8 \mathbf{K}_{Uij}^L (\mathbf{U}_j^{L,p} + \mathbf{U}_j^{L,p+1}) &= \sum_{L=1}^8 (\mathbf{f}_{Ui}^{L,p} + \mathbf{f}_{Ui}^{L,p+1}) \end{aligned} \right\}, \quad (9)$$

(1) 节点位移动力反应的显式

根据时间的中心差分法

$$\left. \begin{aligned} \dot{\mathbf{u}}_i^p &= \frac{1}{2\Delta t} (\mathbf{u}_i^{p+1} - \mathbf{u}_i^{p-1}) \\ \ddot{\mathbf{u}}_i^p &= \frac{1}{\Delta t^2} (\mathbf{u}_i^{p+1} - 2\mathbf{u}_i^p + \mathbf{u}_i^{p-1}) \\ \dot{\mathbf{U}}_i^p &= \frac{1}{2\Delta t} (\mathbf{U}_i^{p+1} - \mathbf{U}_i^{p-1}) \\ \ddot{\mathbf{U}}_i^p &= \frac{1}{\Delta t^2} (\mathbf{U}_i^{p+1} - 2\mathbf{U}_i^p + \mathbf{U}_i^{p-1}) \end{aligned} \right\}, \quad (10)$$

有

$$\left. \begin{aligned} \ddot{\mathbf{u}}_i^p &= \frac{2}{\Delta t^2} (\mathbf{u}_i^{p+1} - \mathbf{u}_i^p) - \frac{2}{\Delta t} \dot{\mathbf{u}}_i^p \\ \ddot{\mathbf{U}}_i^p &= \frac{2}{\Delta t^2} (\mathbf{U}_i^{p+1} - \mathbf{U}_i^p) - \frac{2}{\Delta t} \dot{\mathbf{U}}_i^p \end{aligned} \right\}. \quad (11)$$

将式(11)代入式(8)可以得到用前一时刻的位移和速度表示的当前时刻位移的显式表达式:

$$\begin{aligned} \mathbf{u}_i^{p+1} &= \mathbf{u}_i^p + \Delta t \dot{\mathbf{u}}_i^p - \frac{\Delta t^2}{2} \left(\mathbf{M}_{ui} - \frac{\tilde{\mathbf{M}}_{uUi} \tilde{\mathbf{M}}_{uUi}}{\mathbf{M}_{Ui}} \right)^{-1} \left\{ \left(\sum_{L=1}^8 \sum_{j=1}^8 \mathbf{C}_{ij}^L (\dot{\mathbf{u}}_j^{L,p} - \dot{\mathbf{U}}_j^{L,p}) \right) \left(1 + \frac{\tilde{\mathbf{M}}_{uUi}}{\mathbf{M}_{Ui}} \right) + \sum_{L=1}^8 \sum_{j=1}^8 \mathbf{K}_{uij}^L \mathbf{u}_j^{L,p} \right. \\ &+ \sum_{L=1}^8 \sum_{j=1}^8 \mathbf{K}_{Uij}^L \mathbf{U}_j^{L,p} - \sum_{L=1}^8 \sum_{j=1}^8 \mathbf{K}_{Uij}^L \mathbf{u}_j^{L,p} \frac{\tilde{\mathbf{M}}_{uUi}}{\mathbf{M}_{Ui}} - \sum_{L=1}^8 \sum_{j=1}^8 \mathbf{K}_{Uij}^L \mathbf{U}_j^{L,p} \frac{\tilde{\mathbf{M}}_{uUi}}{\mathbf{M}_{Ui}} - \sum_{L=1}^8 \mathbf{f}_{ui}^{L,p} + \sum_{L=1}^8 \mathbf{f}_{Ui}^{L,p} \frac{\tilde{\mathbf{M}}_{uUi}}{\mathbf{M}_{Ui}} \left. \right\}, \quad (12a) \end{aligned}$$

$$\begin{aligned} \mathbf{U}_i^{p+1} &= \mathbf{U}_i^p + \Delta t \dot{\mathbf{U}}_i^p - \frac{\Delta t^2}{2} \left(\mathbf{M}_{Ui} - \frac{\tilde{\mathbf{M}}_{uUi} \tilde{\mathbf{M}}_{uUi}}{\mathbf{M}_{ui}} \right)^{-1} \left\{ \left(\sum_{L=1}^8 \sum_{j=1}^8 \mathbf{C}_{ij}^L (\dot{\mathbf{u}}_j^{L,p} - \dot{\mathbf{U}}_j^{L,p}) \right) \left(-1 - \frac{\tilde{\mathbf{M}}_{uUi}}{\mathbf{M}_{ui}} \right) - \sum_{L=1}^8 \sum_{j=1}^8 \mathbf{K}_{uij}^L \mathbf{u}_j^{L,p} \right. \\ &\times \frac{\tilde{\mathbf{M}}_{uUi}}{\mathbf{M}_{ui}} - \sum_{L=1}^8 \sum_{j=1}^8 \mathbf{K}_{Uij}^L \mathbf{U}_j^{L,p} \frac{\tilde{\mathbf{M}}_{uUi}}{\mathbf{M}_{ui}} + \sum_{L=1}^8 \sum_{j=1}^8 \mathbf{K}_{Uij}^L \mathbf{u}_j^{L,p} + \sum_{L=1}^8 \sum_{j=1}^8 \mathbf{K}_{Uij}^L \mathbf{U}_j^{L,p} - \sum_{L=1}^8 \mathbf{f}_{Ui}^{L,p} + \sum_{L=1}^8 \mathbf{f}_{ui}^{L,p} \frac{\tilde{\mathbf{M}}_{uUi}}{\mathbf{M}_{ui}} \left. \right\}. \quad (12b) \end{aligned}$$

(2) 节点速度的动力反应显式

根据 Newmark 常平均加速度法,有

$$\left. \begin{aligned} \frac{\ddot{\mathbf{u}}_i^{p+1} + \ddot{\mathbf{u}}_i^p}{2} &= \frac{\dot{\mathbf{u}}_i^{p+1} - \dot{\mathbf{u}}_i^p}{\Delta t} \\ \frac{\dot{\mathbf{u}}_i^{p+1} + \dot{\mathbf{u}}_i^p}{2} &= \frac{\mathbf{u}_i^{p+1} - \mathbf{u}_i^p}{\Delta t} \\ \frac{\ddot{\mathbf{U}}_i^{p+1} + \ddot{\mathbf{U}}_i^p}{2} &= \frac{\dot{\mathbf{U}}_i^{p+1} - \dot{\mathbf{U}}_i^p}{\Delta t} \\ \frac{\dot{\mathbf{U}}_i^{p+1} + \dot{\mathbf{U}}_i^p}{2} &= \frac{\mathbf{U}_i^{p+1} - \mathbf{U}_i^p}{\Delta t} \end{aligned} \right\} \quad (13)$$

将式(13)代入式(12),便可得到用前一时刻的位移、速度以及当前时刻的位移表示的当前时刻速度的显式表达式:

$$\begin{aligned} \dot{\mathbf{u}}_i^{p+1} &= \dot{\mathbf{u}}_i^p - \left(\mathbf{M}_{ui} - \frac{\widetilde{\mathbf{M}}_{uUi} \widetilde{\mathbf{M}}_{uUi}}{\mathbf{M}_{ui}} \right)^{-1} \left\{ \left(\sum_{L=1}^8 \sum_{j=1}^8 \mathbf{C}_{ij}^L (\mathbf{u}_j^{L,p+1} - \mathbf{u}_j^{L,p} - \mathbf{U}_j^{L,p+1} + \mathbf{U}_j^{L,p}) \right) \left(1 + \frac{\widetilde{\mathbf{M}}_{uUi}}{\mathbf{M}_{ui}} \right) \right. \\ &+ \frac{\Delta t}{2} \left[\sum_{L=1}^8 \sum_{j=1}^8 \mathbf{K}_{uuij}^L (\mathbf{u}_j^{L,p+1} + \mathbf{u}_j^{L,p}) + \sum_{L=1}^8 \sum_{j=1}^8 \mathbf{K}_{uUij}^L (\mathbf{U}_j^{L,p+1} + \mathbf{U}_j^{L,p}) - \sum_{L=1}^8 \sum_{j=1}^8 \mathbf{K}_{uUij}^L (\mathbf{u}_j^{L,p+1} + \mathbf{u}_j^{L,p}) \frac{\widetilde{\mathbf{M}}_{uUi}}{\mathbf{M}_{ui}} \right. \\ &\left. - \sum_{L=1}^8 \sum_{j=1}^8 \mathbf{K}_{UUi}^L (\mathbf{U}_j^{L,p+1} + \mathbf{U}_j^{L,p}) \frac{\widetilde{\mathbf{M}}_{uUi}}{\mathbf{M}_{ui}} - \sum_{L=1}^8 (\mathbf{f}_{ui}^{L,p+1} + \mathbf{f}_{ui}^{L,p}) + \sum_{L=1}^8 (\mathbf{f}_{Ui}^{L,p+1} + \mathbf{f}_{Ui}^{L,p}) \frac{\widetilde{\mathbf{M}}_{uUi}}{\mathbf{M}_{ui}} \right] \left. \right\}, \quad (14a) \end{aligned}$$

$$\begin{aligned} \dot{\mathbf{U}}_i^{p+1} &= \dot{\mathbf{U}}_i^p - \left(\mathbf{M}_{Ui} - \frac{\widetilde{\mathbf{M}}_{uUi} \widetilde{\mathbf{M}}_{uUi}}{\mathbf{M}_{ui}} \right)^{-1} \left\{ \left(\sum_{L=1}^8 \sum_{j=1}^8 \mathbf{C}_{ij}^L (\mathbf{u}_j^{L,p+1} - \mathbf{u}_j^{L,p} - \mathbf{U}_j^{L,p+1} + \mathbf{U}_j^{L,p}) \right) \left(-1 - \frac{\widetilde{\mathbf{M}}_{uUi}}{\mathbf{M}_{ui}} \right) \right. \\ &+ \frac{\Delta t}{2} \left[\sum_{L=1}^8 \sum_{j=1}^8 \mathbf{K}_{uUij}^L (\mathbf{u}_j^{L,p+1} + \mathbf{u}_j^{L,p}) + \sum_{L=1}^8 \sum_{j=1}^8 \mathbf{K}_{UUi}^L (\mathbf{U}_j^{L,p+1} + \mathbf{U}_j^{L,p}) - \sum_{L=1}^8 \sum_{j=1}^8 \mathbf{K}_{uuij}^L (\mathbf{u}_j^{L,p+1} + \mathbf{u}_j^{L,p}) \frac{\widetilde{\mathbf{M}}_{uUi}}{\mathbf{M}_{ui}} \right. \\ &\left. - \sum_{L=1}^8 \sum_{j=1}^8 \mathbf{K}_{uUi}^L (\mathbf{U}_j^{L,p+1} + \mathbf{U}_j^{L,p}) \frac{\widetilde{\mathbf{M}}_{uUi}}{\mathbf{M}_{ui}} - \sum_{L=1}^8 (\mathbf{f}_{ui}^{L,p+1} + \mathbf{f}_{ui}^{L,p}) + \sum_{L=1}^8 (\mathbf{f}_{Ui}^{L,p+1} + \mathbf{f}_{Ui}^{L,p}) \frac{\widetilde{\mathbf{M}}_{uUi}}{\mathbf{M}_{ui}} \right] \left. \right\}. \quad (14b) \end{aligned}$$

(3) 节点加速度动力反应的显式

由式(13)可得用前一时刻的速度和此时刻的速度表示的加速度的显式表达式:

$$\left. \begin{aligned} \ddot{\mathbf{u}}_i^{p+1} &= -\ddot{\mathbf{u}}_i^p + 2(\dot{\mathbf{u}}_i^{p+1} - \dot{\mathbf{u}}_i^p)/\Delta t \\ \ddot{\mathbf{U}}_i^{p+1} &= -\ddot{\mathbf{U}}_i^p + 2(\dot{\mathbf{U}}_i^{p+1} - \dot{\mathbf{U}}_i^p)/\Delta t \end{aligned} \right\} \quad (15)$$

式(13), (14), (15)为考虑耦合质量和流体黏性的饱和多孔介质局部节点系下某一节点的动力反应的显式表达式,该节点的动力反应只与相邻节点的动力反应有关.若不考虑耦合质量,即令 $\rho_a = 0$,则有 $\widetilde{\mathbf{M}}_{uUij} = 0$,考虑耦合质量的饱和多孔介质节点的动力反应的显式表达式(16),式(18)可以退化成不考虑耦合质量的饱和多孔介质节点动力反应的显式表达式.

3 饱和多孔介质三维黏弹性动力人工边界

3.1 饱和多孔介质及本构关系

对线弹性饱和多孔介质,本构关系为^[13]

$$\begin{aligned} \sigma_{ij} &= 2\mu e_{ij} + (\lambda e + Q\epsilon)\delta_{ij}, \\ s &= Qe + R\epsilon, \end{aligned} \quad (16)$$

其中, σ_{ij} 为固体骨架应力张量, s 为孔隙流体应力, e, ϵ 分别为固体骨架和孔隙流体的体应变, $e_{ij} = (u_{i,j} + u_{j,i})/2$, δ_{ij} 为 Kronecker 符号, λ, μ, Q, R 为弹性常数.

3.2 人工边界应力条件的推导

3.2.1 人工边界切向应力

因假设孔隙流体无黏性,所以,孔隙流体不承担剪力,在切向只有固体骨架承担剪应力.考虑扩散的球面剪切波,球坐标系球面剪切波动位移的近似解为

$$u = \frac{1}{r} f(r - c_s t). \quad (17)$$

由式(17)所确定的剪应变和剪应力分别为:

$$\begin{aligned} \gamma(r, t) &= \frac{\partial u}{\partial r} - \frac{u}{r} = -\frac{2}{r^2} f(r - c_s t) \\ &+ \frac{1}{r} f'(r - c_s t), \end{aligned} \quad (18)$$

$$\tau(r, t) = \mu \gamma = \mu \left[-\frac{2}{r^2} f(r - c_s t) + \frac{1}{r} f'(r - c_s t) \right]. \quad (19)$$

在坐标 r 处质点的运动速度为

$$\dot{u} = \frac{\partial u(r,t)}{\partial t} = -\frac{c_s}{r} f'(r - c_s t). \quad (20)$$

由式(17)、(18)、(19)可得在波阵面上

$$\tau(r,t) = -\frac{2\mu}{r} u(r,t) - \frac{\mu}{c_s} \dot{u}(r,t). \quad (21)$$

式(21)即为三维切向人工边界方程,该方程给出了波阵面上切向应力与位移的关系式。

对于如式(21)所示的三维切向边界方程,容易证明该方程等价于并联的弹簧-阻尼器系统,对应物理元件的参数为

$$k = \frac{2\mu}{r}, c = \frac{\mu}{c_s}. \quad (22)$$

其中, k 为弹簧刚度系数, c 为黏性阻尼系数。

3.2.2 人工边界法向应力

忽略饱和多孔介质中慢 P 波的影响,只考虑球面快 P 波^[9],球坐标系下其波动方程为

$$\frac{\partial^2(r\phi)}{\partial r^2} = \frac{1}{c_p^2} \frac{\partial^2(r\phi)}{\partial t^2}, \quad (23)$$

其中 ϕ 为位移势函数, c_p 为饱和多孔介质的快 P 波波速, r 为径向坐标. 方程(23)的通解可表示为

$$\phi(r,t) = \frac{1}{r} f(r - c_p t) + \frac{1}{r} g(r + c_p t), \quad (24)$$

式中 $f(\cdot)$ 和 $g(\cdot)$ 为任意函数,分别表示外行扩散波和内行会聚波。

考虑外行扩散波

$$\phi(r,t) = \frac{1}{r} f(r - c_p t). \quad (25)$$

首先分析固体骨架的法向应力,固体骨架法向位移为

$$u = \frac{\partial \phi}{\partial r} = \frac{1}{r} f'(r - c_p t) - \frac{1}{r^2} f(r - c_p t), \quad (26)$$

法向与切向应变为

$$\epsilon_r = \frac{\partial u}{\partial r}, \quad (27)$$

$$\epsilon_\theta = \frac{u}{r}. \quad (28)$$

由式(16)固体骨架法向应力为

$$\sigma_r(r,t) = (\lambda + 2\mu + Q\eta_1)(\epsilon_r + \epsilon_\theta) - 2\mu\epsilon_\theta, \quad (29)$$

其中, η_1 为液相参与系数。

固体骨架速度、加速度为

$$\dot{u} = -\frac{c_p}{r} f''(r - c_p t) + \frac{c_p}{r^2} f'(r - c_p t), \quad (30)$$

$$\ddot{u} = \frac{c_p^2}{r} f'''(r - c_p t) - \frac{c_p^2}{r^2} f''(r - c_p t). \quad (31)$$

对式(26)求导可得

$$\begin{aligned} \frac{\partial u}{\partial r} &= \frac{1}{r} f''(r - c_p t) - \frac{2}{r^2} f'(r - c_p t) \\ &+ \frac{2}{r^3} f(r - c_p t), \end{aligned} \quad (32)$$

$$\frac{u}{r} = \frac{1}{r^2} f'(r - c_p t) - \frac{1}{r^3} f(r - c_p t), \quad (33)$$

令 $G = \lambda + Q\eta_1 + 4\mu$, $\rho c_x^2 = \lambda + 2\mu + Q\eta_1$, 将式(26)、(27)和(28)代入式(29),得

$$\begin{aligned} \sigma_r(r,t) &= \frac{\rho c_x^2}{r} f''(r - c_p t) - \frac{G}{r^2} f'(r - c_p t) \\ &+ \frac{G}{r^3} f(r - c_p t), \end{aligned} \quad (34a)$$

$$\begin{aligned} \frac{\partial \sigma_r(r,t)}{\partial t} &= -c_p \frac{\rho c_x^2}{r} f'''(r - c_p t) + c_p \frac{G}{r^2} f''(r - c_p t) \\ &- c_p \frac{G}{r^3} f'(r - c_p t). \end{aligned} \quad (34b)$$

将式(34b)乘以系数 $\frac{r}{c_p}$, 得到

$$\begin{aligned} \frac{r}{c_p} \frac{\partial \sigma_r(r,t)}{\partial t} &= -\rho c_x^2 f'''(r - c_p t) + \frac{G}{r} f''(r - c_p t) \\ &- \frac{G}{r^2} f'(r - c_p t), \end{aligned} \quad (34c)$$

将式(34c)与式(34a)相加,并结合式(30)、(31)得

$$\sigma_r + \frac{r}{c_p} \frac{\partial \sigma_r}{\partial t} = -\frac{G}{r} \left(u + \frac{r}{c_p} \dot{u} + \frac{r^2 \rho c_x^2}{G c_p^2} \ddot{u} \right). \quad (35)$$

式(35)与图 1 所示的弹簧-阻尼-质量模型的动力系统运动方程式(36)等价

$$f_1 + \frac{m}{c} \dot{f}_1 = k \left(u_1 + \frac{m}{c} \dot{u}_1 + \frac{m}{k} \ddot{u}_1 \right). \quad (36)$$

在人工边界 $r = r_b$ 处,等效弹簧、黏性阻尼和质量系数为

$$\begin{cases} k = \frac{G}{r_b} = \frac{\lambda + Q\eta_1 + 4\mu}{r_b} \\ c = \frac{\lambda + 2\mu + Q\eta_1}{c_p} \\ m = \frac{(\lambda + 2\mu + Q\eta_1)r_b}{c_p^2} \end{cases}. \quad (37)$$

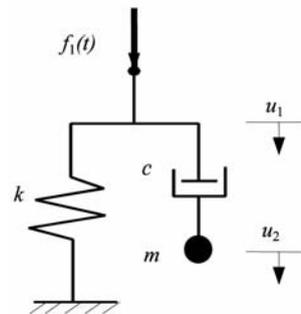


图 1 弹簧-阻尼-质量模型
Fig. 1 Spring-damp-mass model

将图 1 中的质量忽略, 将阻尼的另一端直接固定, 成为弹簧-阻尼模型, 如图 2 所示. 这样简化并不明显影响人工边界的精度, 但给实际应用带来极大的方便^[15]. 简化后的三维黏弹性人工边界如图 3 所示, 图中坐标 x, y 为沿人工边界的切向方向, z 为沿人工边界的法向方向.

对于孔隙流体, 因忽略慢 P 波, $u = \frac{U}{\eta_1}, \dot{u} = \frac{\dot{U}}{\eta_1}$ (η_1 为液相参与系数), 由式 (16), 孔隙流体在人工边界法向应力为

$$s = (Q + R\eta_1)e. \tag{38}$$

由式 (29) 得

$$e = \frac{(\sigma_r(r, t) + 2\mu \frac{u}{r})}{(\lambda + 2\mu + Q\eta_1)}, \tag{39}$$

又由式 (26)~(29) 得

$$\sigma_r(r, t) = -\frac{\lambda + 4\mu + Q\eta_1}{r}u - \frac{(\lambda + 2\mu + Q\eta_1)}{c_p}\dot{u}. \tag{40}$$

将式 (39)、(40) 代入式 (38), 并注意到 $u = U/\eta_1, \dot{u} = \dot{U}/\eta_1$, 则在人工边界 $r = r_b$ 的流体法向应力为

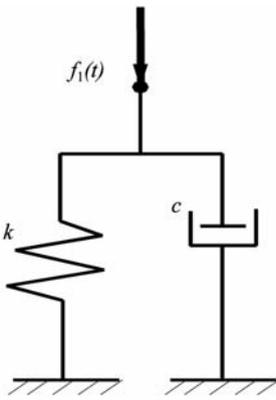


图 2 弹簧-阻尼模型
Fig. 2 Spring-damp model

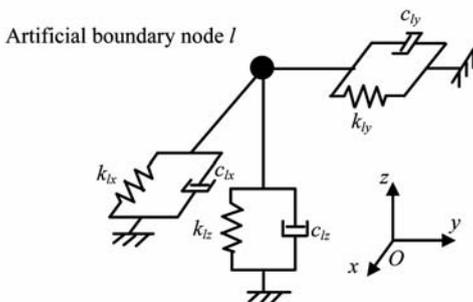


图 3 三维黏弹性人工边界示意图
Fig. 3 Three dimensional viscous-spring boundary

$$s = -\frac{Q + R\eta_1}{\eta_1} \left(\frac{U}{r_b} + \frac{\dot{U}}{c_p} \right). \tag{41}$$

其中, U, \dot{U} 为人工边界处孔隙流体的法向位移和速度. 设 $k^l = \frac{Q + R\eta_1}{\eta_1 r_b}$, 为孔隙流体等效弹簧系数; $c^l = \frac{Q + R\eta_1}{\eta_1 c_p}$, 为孔隙流体黏滞阻尼系数.

3.2.3 直角坐标系下人工边界应力条件

假设在半空间问题分析中采用直角坐标系下的矩形人工边界. 球面人工边界上的法向矢量与切向矢量构成局部坐标系, 固体骨架应力矢量用矩阵表达为

$$\sigma^l = K^l z^l + C^l \dot{z}^l, \tag{42}$$

其中

$$\sigma^l = (\sigma_r, \sigma_\varphi, \sigma_\theta)^T, K^l = \begin{bmatrix} k_r & 0 & 0 \\ 0 & k_\varphi & 0 \\ 0 & 0 & k_\theta \end{bmatrix},$$

$$C^l = \begin{bmatrix} c_r & 0 & 0 \\ 0 & c_\varphi & 0 \\ 0 & 0 & c_\theta \end{bmatrix}; z^l = (u, v, w)^T,$$

z^l 为位移矢量, $k_\varphi, c_\varphi, k_\theta, c_\theta$ 分别为固体骨架切向弹簧刚度系数和黏性阻尼系数, k_r, c_r 分别为固体骨架径向弹簧刚度系数和黏性阻尼系数.

局部坐标系下的应力与位移矢量与直角坐标系下的应力与位移矢量的变换关系为

$$\sigma^l = T\sigma, \tag{43}$$

$$z^l = Tz, \tag{44}$$

其中,

$$\sigma = (\sigma_x, \sigma_y, \sigma_z)^T, z = (u_x, u_y, u_z)^T,$$

T 为坐标转换矩阵. 将式 (43)、(44) 代入式 (42), 得直角坐标系下的应力矢量为

$$\sigma = Kz + C\dot{z}. \tag{45}$$

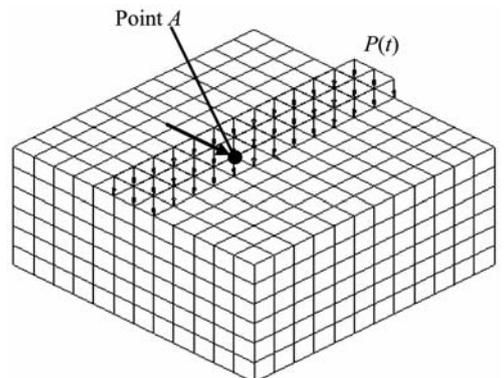


图 4 有限元三维模型
Fig. 4 The 3D finite element model

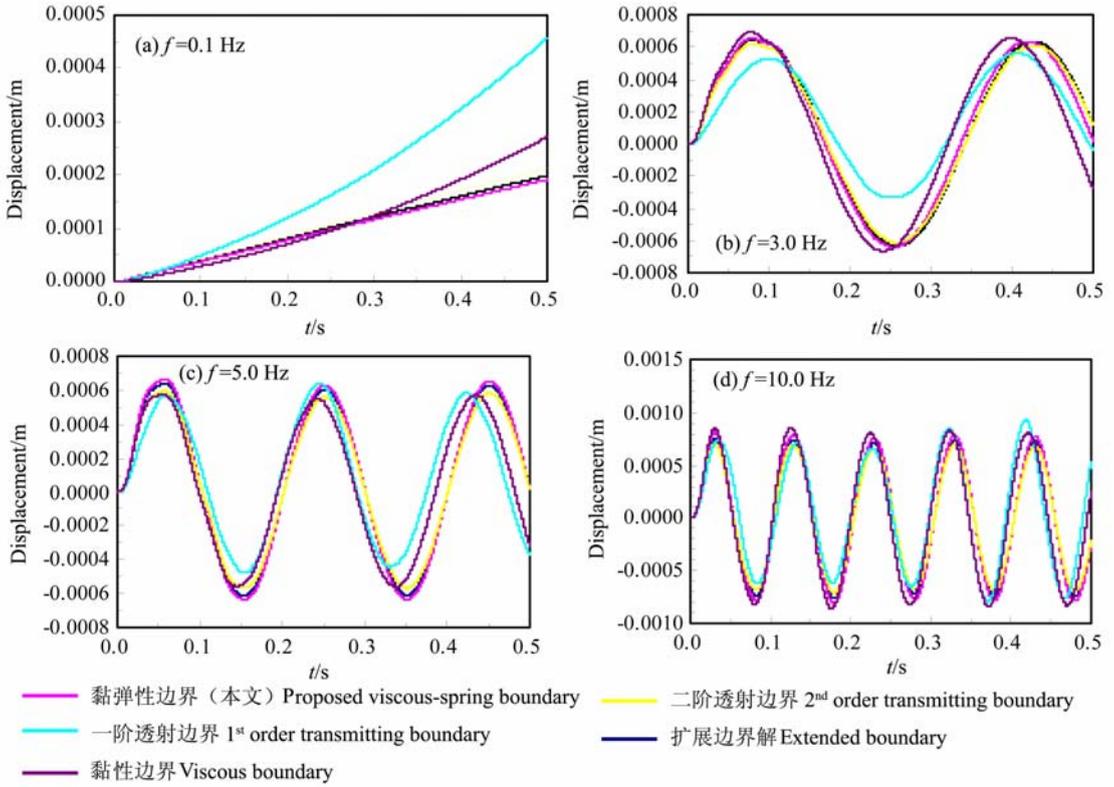


图 5 A 点在不同频率水平荷载下的水平位移历程

Fig. 5 Horizontal displacements at point A with different frequencies under horizontal load

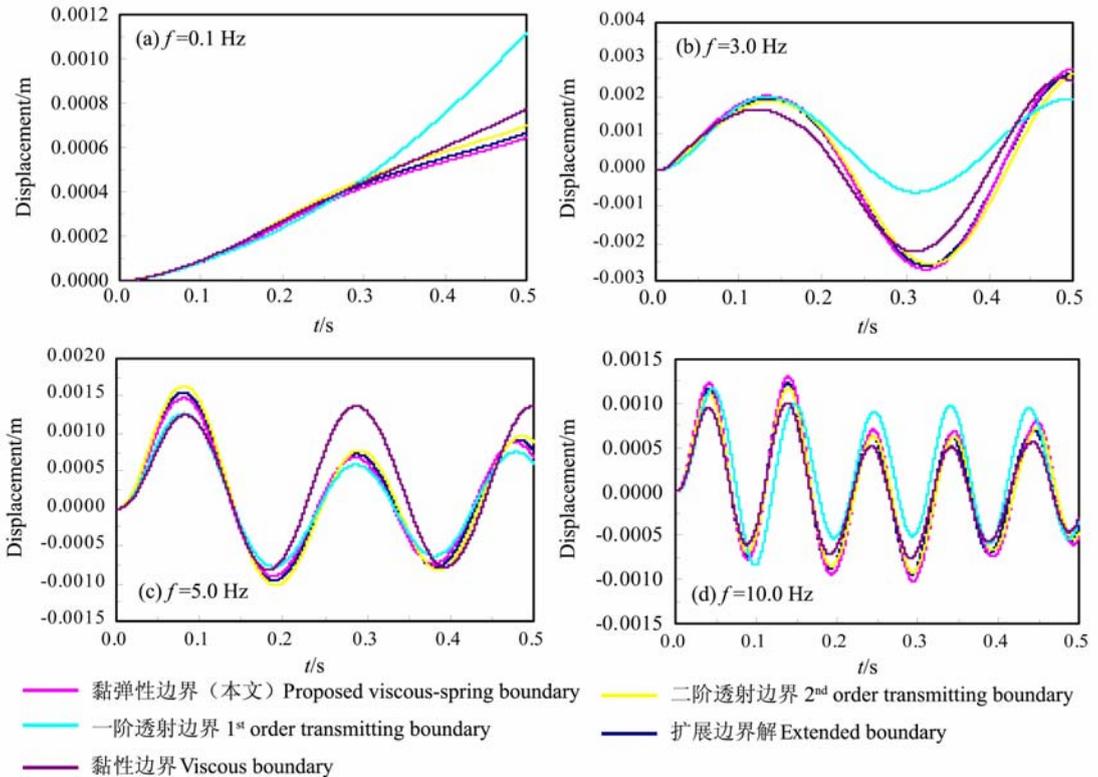


图 6 A 点在不同频率竖向荷载下的竖向位移历程

Fig. 6 Vertical displacements at point A with different frequencies under vertical load

表 1 材料特性参数
Table 1 Basic properties of the material

λ/Pa	μ/Pa	n	$\rho_s/(\text{kg}/\text{m}^3)$	$\rho_l/(\text{kg}/\text{m}^3)$	$\rho/(\text{kg}/\text{m}^3)$	Q/Pa	R/Pa
2.919×10^8	1.250×10^8	0.33	0.3101	0.2977	0.301	1.541×10^8	1.535×10^8

其中

$$\mathbf{K} = \mathbf{T}^{-1} \mathbf{K}' \mathbf{T}, \mathbf{C} = \mathbf{T}^{-1} \mathbf{C}' \mathbf{T},$$

$$\mathbf{T} = \begin{bmatrix} \sin\varphi \cos\theta & \sin\varphi \sin\theta & \cos\varphi \\ \cos\varphi \cos\theta & \cos\varphi \sin\theta & -\sin\varphi \\ -\sin\varphi \sin\theta & \sin\varphi \cos\theta & 0 \end{bmatrix}.$$

孔隙流体应力在直角坐标系下表达为

$$s_i = k' U_i + c' \dot{U}_i (i = x, y, z). \quad (46)$$

式(45)、(46)即为直角坐标系下矩形平面人工边界上的应力表达式。 $\boldsymbol{\sigma}$ 和 s_i 分别为人工边界上某一点的固体骨架和孔隙流体的应力矢量,在有限元计算中,可简单地将边界上节点应力乘以相邻四个单元面积的平均值,作为节点集中力列入到节点动力平衡方程中,并集装到总体刚度矩阵和阻尼矩阵中。

4 数值计算

算例 1、2 分别给出两种不同荷载形式下地面一点的位移曲线,算例中把应用本文提出的人工边界条件的数值计算结果与应用黏性边界^[3]及一、二阶透射边界^[14]、扩展人工边界的解进行了对比分析。其中,扩展有限元解是将人工边界远置,使得在计算时间段内从人工边界反射回来的波不能到达所考虑的点或局部区域。

算例 1: 三维半空间情况下,在自由面中央 A 点作用一水平集中动荷载,见图 4, $P(t) = P_0 \sin\omega t$, $P_0 = 1 \text{ N}$, 地震工程感兴趣的频段为: 0.1~10 Hz。选择频率分别为 0.1 Hz, 1 Hz, 3 Hz, 5 Hz。计算区域: 12 m×12 m×6 m, 采用立方体单元离散计算区域, 假设固相不可压缩, 材料参数见表 1。计算在水平集中力作用下, 作用点处水平位移时程曲线, 计算时间为 0.5 s, 见图 5。图中分别给出了本文边界、黏性边界、一、二阶透射边界对应的数值解, 精确解采用扩展有限元解。采用本文提出的有限元程序进行计算。图 5 表明, 在水平动荷载作用下, 尽管应用本文提出的人工边界条件的数值计算结果与扩展有限元解之间略有误差, 但它的数值解与扩展有限元解是最接近的, 而且不论动载是在低频 ($f = 0.1 \text{ Hz}$) 或高频 ($f = 10.0 \text{ Hz}$), 其数值计算结果很稳定; 一阶透射边界解与扩展边界解相差较远, 这是由于本

模型人工边界尺寸较小, 一阶透射边界结果受不同模型影响明显, 人工边界尺寸越大精度越高, 这给透射边界应用带来不便。

算例 2: 如图 4 所示, 自由面有一宽度 2 m 竖向作用的条形简谐变化荷载, $P(t) = P_0 \sin\omega t$, $P_0 = 1 \text{ N}$ 。仍选择频率分为: 0.1 Hz, 1 Hz, 3 Hz, 5 Hz, 计算域的尺寸和材料常数同算例 1。计算得到地表正中央 A 点在不同荷载频率和人工边界条件下的竖向位移时程曲线, 计算时间为 0.5 s, 见图 6。由图可见, 在竖向动荷载作用下, 尽管本文黏弹性人工边界的数值计算结果与扩展有限元解之间略有误差, 但它的数值解与扩展有限元解是接近的, 低频 ($f = 0.1 \text{ Hz}$) 时比二阶透射边界的精度高, 较高频率 ($f = 10.0 \text{ Hz}$) 时与二阶透射边界的精度相当。而且不论动载是在低频或较高频率, 其数值计算结果很稳定。

5 结 语

本文提出了饱和多孔介质的三维黏弹性人工边界和饱和多孔介质三维动力反应分析的显式有限元法, 给出计算公式, 开发了实现该有限元方法的程序。数值计算表明: 本文提出饱和多孔介质三维黏弹性人工边界具有较好的精度和稳定性, 应用简单, 便于有限元数值计算; 有限元程序具有较好的精度和稳定性, 运算速度快, 能达到较好的数值分析效果。

参考文献(References)

- [1] Modaresi H, Benzenati I. An absorbing boundary element for dynamic analysis of two-phase media. In: Proceedings of the 10th World Conference on Earthquake Engineering, 1992. 1157~1161
- [2] Degrande G, De Roeck G. Absorbing boundary condition for wave propagation in saturated poroelastic media - Part I: Formulation and efficiency evaluation. *Soil Dynamics and Earthquake Engineering*, 1993, **12**: 411~421
- [3] Akiyoshi T, Fuchida K, Fang H L. Absorbing boundary conditions for dynamic analysis of fluid-saturated porous media. *Soil Dynamics and Earthquake Engineering*, 1994, **13**: 387~397
- [4] Gajo A, Saetta A, Vitaliani R. Silent boundary conditions for wave propagation in saturated porous media. *International*

- Journal for Numerical and Analytical Methods in Geomechanics*, 1996, **20**: 253~273
- [5] Akiyoshi T, Sun X, Fuchida K. General absorbing boundary conditions for dynamic analysis of fluid-saturated porous media. *Soil Dynamics and Earthquake Engineering*, 1998, **17**: 397~406
- [6] 邵秀民, 蓝志凌. 流体饱和多孔介质波动方程的有限元解法. *地球物理学报*, 2000, **43**(2): 264~278
Shao X M, Lan Z L. Finite element methods for the equations of waves in fluid-saturated porous media. *Chinese J. Geophys.* (in Chinese), 2000, **43**(2): 264~278
- [7] Zerfa Z, Loret B. A viscous boundary for transient analyses of saturated porous media. *Earthquake Engineering and Structural Dynamics*, 2004, **33**: 89~110
- [8] Bowen R M. Incompressible porous media by use of the theory of mixtures. *Inter. J. Eng. Sci.*, 1980, **18**: 19~45
- [9] 刘光磊, 宋二祥. 饱和无限地基数值模拟的黏弹性传输边界. *岩土工程学报*, 2006, **28**(12): 2128~2133
Liu G L, Song E X. Visco-elastic transmitting boundary for numerical analysis of infinite saturated soil foundation. *Chinese Journal of Geotechnical Engineering* (in Chinese), 2006, **28**(12): 2128~2133
- [10] 王子辉, 赵成刚, 董亮. 流体饱和多孔介质黏弹性动力人工边界. *力学学报*, 2006, **38**(5): 605~611
Wang Z H, Zhao C G, Dong L. A viscous-spring dynamic artificial boundary for saturated porous media. *Chinese Journal of Theoretical and Applied Mechanics* (in Chinese), 2006, **38**(5): 605~611
- [11] 杜修力, 李立云. 饱和多孔介质近场波动分析的一种黏弹性人工边界. *地球物理学报*, 2008, **51**(2): 575~581
Du X L, Li L Y. A viscous spring artificial boundary for near field wave analysis in saturated porous media. *Chinese J. Geophys.* (in Chinese), 2008, **51**(2): 575~581
- [12] 赵成刚, 王进廷, 史培新等. 流体饱和两相多孔介质动力反应分析的显式有限元法. *岩土工程学报*, 2001, **23**(2): 178~182
Zhao C G, Wang J T, Shi P X, et al. Dynamic analysis of fluid-saturated porous media by using explicit finite element method. *Chinese Journal of Geotechnical Engineering* (in Chinese), 2001, **23**(2): 178~182
- [13] Biot M A. Theory of propagation of elastic waves in a fluid-saturated porous solid. I. Low-frequency range. *The Journal of the Acoustical Society of America*, 1956, **28**: 168
- [14] 廖振鹏. 工程波动理论导论. 北京: 科学出版社, 2002
Liao Z P. Introduction to Wave Motion Theories in Engineering (in Chinese). Beijing: Science Press, 2002
- [15] 王振宇. 大型结构—地基系统动力反应计算理论及其应用研究[博士论文]. 北京: 清华大学, 2002
Wang Z Y. Computational theory of dynamic response of large structure-soil systems and its application [Ph. D. thesis]. Beijing: Tsinghua University, 2002

(本文编辑 胡素芳)